AD_____

Award Number: W81XWH-12-1-0303

TITLE: Piezoelectric Composite Micromachined Multifrequency Transducers For High-Resolution, High-Contrast Ultrasound Imaging For Improved Prostate Cancer Assessment

PRINCIPAL INVESTIGATOR: Paul A. Dayton

CONTRACTING ORGANIZATION: University of North Carolina at Chapel Hill
Chapel Hill, NC 27599-5023

REPORT DATE: August 2015

TYPE OF REPORT: Annual

PREPARED FOR: U.S. Army Medical Research and Materiel Command
Fort Detrick, Maryland 21702-5012

REPORT DOCUMENTATION PAGE

Form Approved
OMB No. 0704-0188

1. REPORT DATE	2. REPORT TYPE	3. DATES COVERED
August 2015	Annual	1 Aug 2014 – 31 Jul 2015

4. TITLE AND SUBTITLE

Piezoelectric Composite Micromachined Multifrequency Transducers For High-Resolution, High-Contrast Ultrasound Imaging For Improved Prostate Cancer Assessment

5a. CONTRACT NUMBER

5b. GRANT NUMBER

W81XWH-12-1-0303

5c. PROGRAM ELEMENT NUMBER

6. AUTHOR(S)

Paul A. Dayton Team members Sibo Li, Jinwook Kim, and Sandeep Kasoji, co-PI Xiaoning Jiang.

E-Mail: padayton@email.unc.edu

5d. PROJECT NUMBER

5e. TASK NUMBER

5f. WORK UNIT NUMBER

7. PERFORMING ORGANIZATION NAME(S) AND ADDRESS(ES)

University of North Carolina at Chapel Hill
Office Building, Suite 2200
104 Airport Drive, CB#1350
Chapel Hill, NC 27599-1350

Subcontracting:
North Carolina State University
2701 Sullivan Drive, Suite 240
Raleigh, NC 27695

8. PERFORMING ORGANIZATION REPORT NUMBER

9. SPONSORING / MONITORING AGENCY NAME(S) AND ADDRESS(ES)

U.S. Army Medical Research and Materiel Command
Fort Detrick, Maryland 21702-5012

10. SPONSOR/MONITOR'S ACRONYM(S)

11. SPONSOR/MONITOR'S REPORT NUMBER(S)

12. DISTRIBUTION / AVAILABILITY STATEMENT

Approved for Public Release; Distribution Unlimited

13. SUPPLEMENTARY NOTES

14. ABSTRACT

The objective of this proposal is to develop new technology for substantially improving the sensitivity of ultrasound to prostate cancer. This technology will be enabled by recent advances in ultrasound transducer fabrication techniques and ultrasound contrast imaging approaches. We hypothesize that a transrectal ultrasound probe utilizing a novel dual-frequency ultra-broadband approach will provide a new highly-sensitive diagnostic technique for prostate cancer imaging.

Aim 1) Develop a new type of dual-frequency PC-MUT co-linear array with broad bandwidth to enable a new dual-frequency imaging technology for high-resolution, high sensitivity nonlinear transrectal contrast imaging. This probe will be fabricated using a new piezoelectric composite micromachined ultrasound transducer technology (PC-MUT), and by utilizing through-waver-via based multilayering technology. The final result will be a co-linear 2-D array configuration utilizing row-column electrodes.

Aim 2) Assess the performance of new prototype array and imaging capability in (a) tissue mimicking and microvascular phantoms and in (b) a standard animal model of prostate cancer. In the preliminary in-vitro study, imaging resolution, contrast to tissue ratio, and lesion detectability will be assessed relative to a Siemens EV-8C4 transrectal ultrasound probe. In the in-vivo study, molecular imaging and microvascular mapping will both be performed to assess the probe's ability

Progress to date has included development of prototype single and multi-element array dual frequency transducers designed towards prostate imaging. Prototypes have been fabricated and tested and contrast imaging has been performed in phantoms using single element transducers as well as linear arrays. The prototyped single element dual frequency (2MHz/14 MHz) transducer was tested successfully for detection of super-harmonic signals from microbubbles. A 24/54 element dual-frequency (2 MHz/12 MHz) sub linear array was fabricated and successfully tested for micro bubble contrast imaging. Finally, a full aperture array with finer pitch size was developed and characterized.

15. SUBJECT TERMS

Nothing Listed

16. SECURITY CLASSIFICATION OF:			**17. LIMITATION OF ABSTRACT**	**18. NUMBER OF PAGES**	**19a. NAME OF RESPONSIBLE PERSON**
					USAMRMC
a. REPORT	**b. ABSTRACT**	**c. THIS PAGE**			**19b. TELEPHONE NUMBER** *(include area code)*
U	U	U	UU	21	

Table of Contents

Introduction

Prostate cancer is challenging to assess with standard ultrasound. Our team has recently demonstrated a new approach of ultrasound imaging that uses a contrast agent with a dual-frequency transducer to produce high resolution images of microvascular structure. It is hypothesized that microvascular structure and density are related to degree of cancer, and that this new imaging approach may help us assess prostate cancer. However, to date, there are no dual-frequency transducers designed for prostate cancer imaging that can perform this high-resolution imaging approach. The objective of the proposed research is to design and test a dual-frequency transducer specifically for prostate cancer imaging using contrast agents.

Keywords

Ultrasound, acoustic angiography, dual-frequency, transducer, contrast agents, prostate

Acronyms

PC-MUT	Piezo Composite Micromachined Ultrasound Transducer
TRUS	Trans Rectal Ultrasound
KLM	Krimholtz–Leedom–Matthaei
PMN-PT	Lead Magnesium Niobate-Lead Titanate
TWV	Through-wafer-vias
EWOF	Extension without funds

Overall Project Summary

The original tasks as proposed are listed in light blue (unchanged). ***New progress for year 3 is presented in black.***

Aim 1) Develop a new type of dual-frequency PC-MUT co-linear array with broad bandwidth to enable a new dual-frequency imaging technology for high-resolution, high sensitivity nonlinear transrectal contrast imaging.

Task 1 PC-MUT co-linear array design (Months 1-12)
Extensive modeling will be performed to design 1D and 2D dual frequency (5 MHz/20 MHz) co-linear arrays. The pressure field with amplitude > 2 MPa at a few cm depth is expected from a 5 MHz array for effective microbubble excitation. A 20 MHz PC-MUT with -6dB bandwidth > 90% will be developed as the receiver and integrated with the 5 MHz transmitter for TRUS contrast imaging.

Methods and Results for Task 1: Progress towards Task 1 was reported in the prior progress reports.

Task 2 Dual frequency PC-MUT co-linear array fabrication (Months 4-21)
Dual frequency co-linear array fabrication processes will be developed under this task for dual frequency co-linear array prototyping. At the end of this task, a co-linear array with 64-element 5 MHz 1D array and 128-element 20 MHz 1D array will be fabricated for demonstration of dual frequency PC-MUT co-linear array technology.

Subtask 2.1 1-3 piezocomposite fabrication (Months 3-6)
The fabrication of 20 MHz PC-MUT receivers will follow the standard PC-MUT fabrication process. For the 5 MHz PC-MUT transmitter, PIN-PMN-PT 1-3 composite will be fabricated using dice-and-fill process. The electromechanical coupling coefficient of fabricated 1-3 piezo composites are expected to be > 0.75.

Subtask 2.2 Multilayering process (Months 6-12)
Conductive through-wafer-vias (TWV) process will be developed for multilayer transducer demonstration. Bonding process for single layer and multilayer dual frequency co-linear array fabrication will be developed under this subtask.

Subtask 2.3 Dual frequency co-linear array prototyping (Months 12-21)
The 5 MHz composite layer will be fabricated first, followed by attachment of the 20 MHz receiver and matching layers. The bonded co-linear array acoustic stack will then be wired and tested.

Methods and Results for Task 2:

Sub-array fabrication

Table 1 Design parameters of elements in 2-12 sub-array

	2.2 MHz	**12 MHz**
Aperture	12 mm by 540 μm	6 mm by 270 μm
Backing Layer	-	Alumina (25μm) / Ni (80 μm)
Active Material	1-3 composite (770 μm)	PMN-PT (100 μm)
Matching Layer	Alumina (200 μm)	Alumina (30 μm)

Based on simulations and results from the single element tests, years 2 and 3 have included progress towards the design of the final a dual frequency linear array. These studies included the fabrication and testing subarrays to verify desired functionality, and then culminated in a fabrication of a full array prototype. Our final designs utilize configurations of 2-3 MHz transmit capability and 12-18 MHz receive. These parameters were a lower frequency range than originally proposed, but prior experiments and simulations suggested they would provide a higher contrast to noise ratio. An example sub aperture array first fabricated for initial imaging characterization and contrast tests is described in Figure 1 and Table 1. For transducer element characterization, impedance and pulse/echo tests were conducted. For imaging tests, two scenarios were considered, 1) high frequency B-mode for tissue imaging; and 2) transmit low and receive high mode for test for super harmonic contrast imaging.

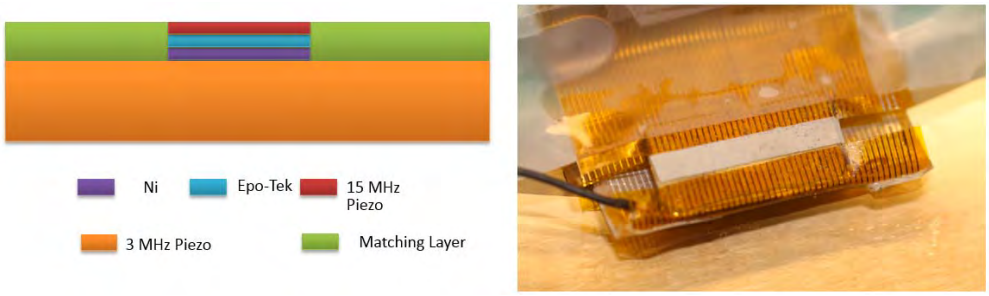

Figure 1. Schematic of dual frequency array ultrasound and a photograph of the sub-array probe.

Full array fabrication

Table 2 Specifications of the full array

Aperture	*8 mm by 20 mm*
Low Frequency Tx	3.5 MHz (3 MHz)
Tx Number	64
Tx Pitch	270 mm
Tx Width	240 mm
Tx Thickness	530 mm
High Frequency Rx	20 MHz (18 MHz)

Rx Number	128
Rx Pitch	135 mm
Rx Width	80 mm
Rx Thickness	105 mm

The full array was fabricated with a stack structure similar to the sub linear array. To further improve imaging performance, the pitch size was reduced and element number was increased. The prototyped probe was equipped with 64/128 elements, 270/135 μm dual layer array (Figure 2). The design details can be found in Table 2.

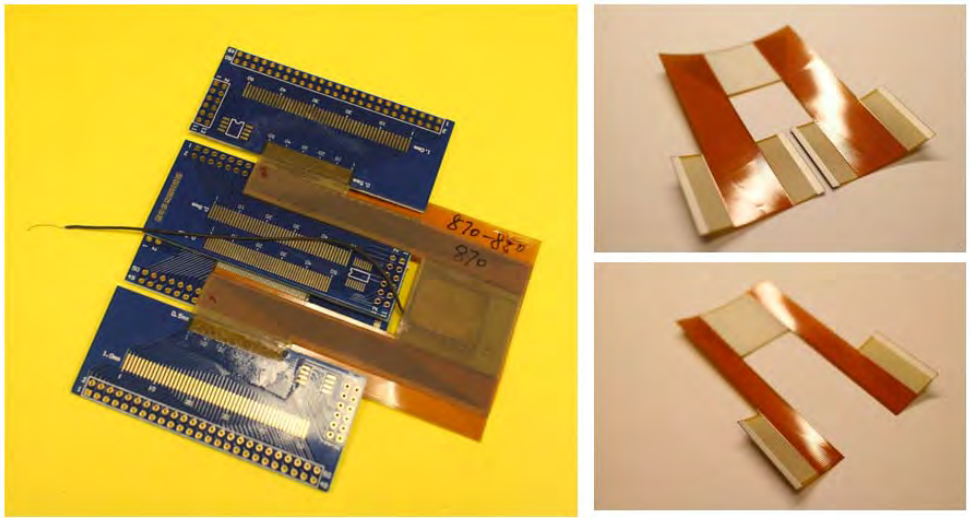

Figure 2. A photograph of full array probe with flex circuit and PCB (left) and two flex circuit prototype for low and high components (right).

Task 3 Characterization of dual frequency PC-MUT co-linear array (Months 15-27)

Electrical and acoustic characterizations will be performed under this task to evaluate the prototyped dual frequency co-linear array.

Subtask 3.1 Electrical characterization (Months 15-21)

Resonant frequency, capacitance, and electrical impedance of single element and a group of elements will be measured using an impedance analyzer. The measured values will be compared with the modeling results.

Subtask 3.2 Acoustic characterization (Months 21-27)

Transducer characterization will be performed under this subtask. The prototype array will be driven with the multi-channel Verasonics programmable ultrasound pulser/receiver). Pulse-echo and hydrophone (HNC-0200, Onda Corp) characterization will be performed in water tank to obtain the transmission characteristics of the 5 MHz transmitter, and the receiving sensitivity and bandwidth of the 20 MHz receiver.

Methods and Results for Task 3:

Sub-array characterization

The electrical impedance of selected subarray elements were measured using an Agilent 4294A precision impedance analyzer (Agilent Technologies Inc., Santa Clara, CA). The transmission element exhibits the fundamental resonant frequency of 2.2 MHz, and the resonant frequency of the receiving part is 12 MHz (Figure 3).

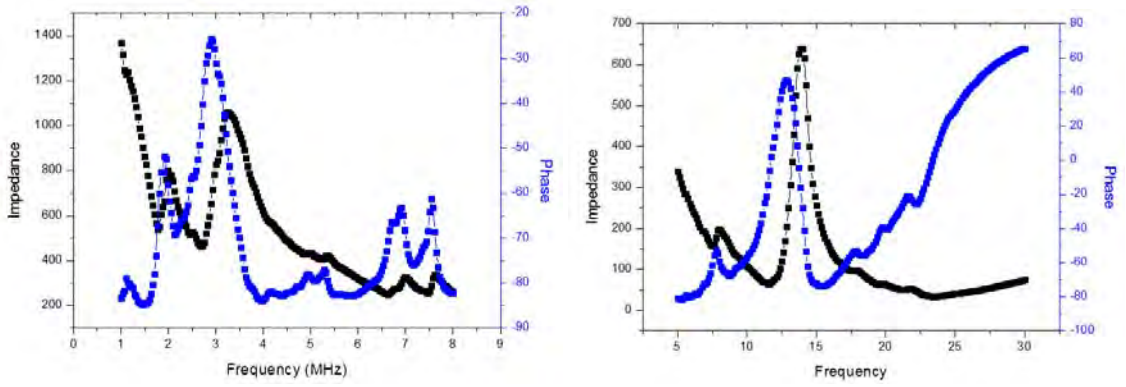

Figure 3. Electrical response of elements in a sub-array for transmission (left) and receiving (right), respectively.

The transmitting and receiving performance of selected elements were tested using a pulser/receiver (5900PR and 5077PR, Panametrics Inc., Waltham, MA). During the pulse-echo tests, a stainless steel block was used as a target and positioned at certain distance away from the transducer. The 2.2 MHz transmitter and the 12 MHz receiver were tested with two different pulser/receivers considering their different usable frequency ranges. The low transmission element was excited by 200 V pulse, and showed a peak-to-peak voltage of 1 V and -6 dB bandwidth of ~45%. The receiving element was excited by 1 μJ pulse and showed ~ 30 mVpp response and ~50% in -6 dB bandwidth , respectively (Figure 4).

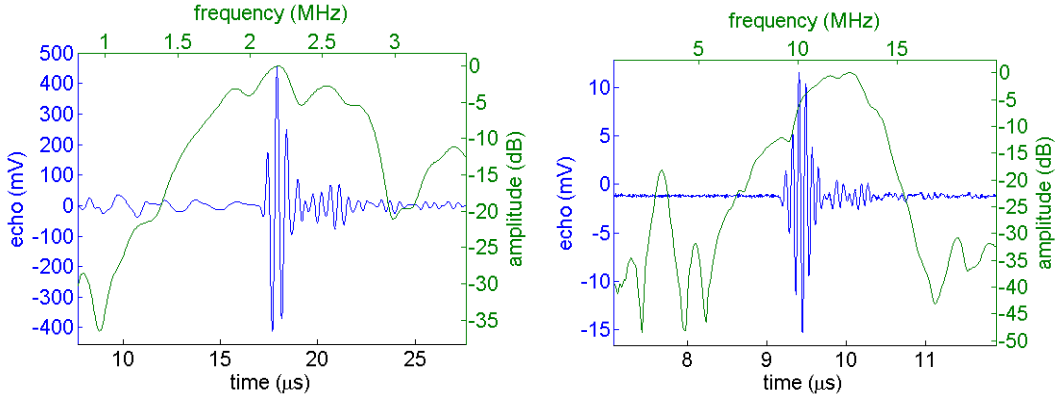

Figure 4. Pulse-echo responses of the sub-array elements at transmission (left) and receiving (right) modes.

Full array Characterization

The electrical impedance of selected elements were measured using an Agilent 4294A precision impedance analyzer (Agilent Technologies Inc., Santa Clara, CA). The transmission elements exhibited a fundamental resonant frequency of 3 MHz, and the resonant frequency of the receiving elements is 17 MHz (Figure 5).

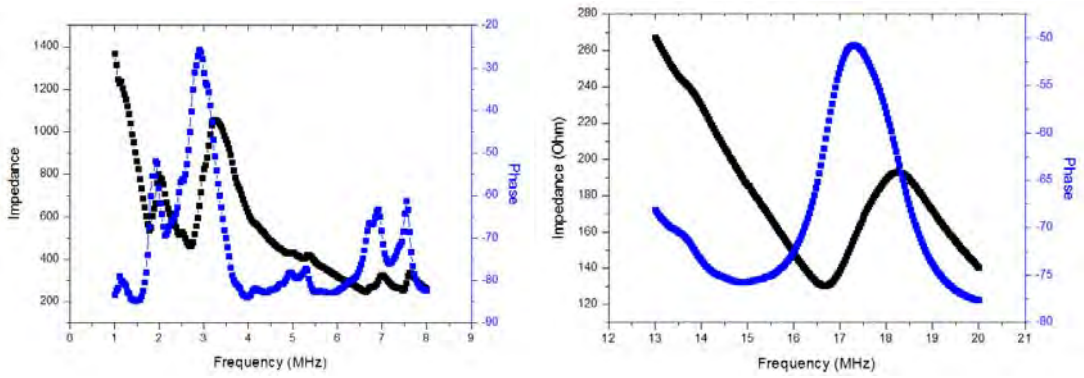

Figure 5. Electrical impedance and phase spectra of the full array elements at transmission (left) and receiving (right).

The pulse-echo tests were conducted for selected transmitting and receiving elements using a pulser/receiver (5900PR and 5077PR, Panametrics Inc., Waltham, MA). During the pulse-echo test, a stainless steel block, positioned at certain distance away from the transducer, was used as a target. The 3 MHz transmitter and the 18 MHz receiver were tested with two different pulser/receivers considering their different usable frequency ranges. The low transmission element was excited by 100 V pulse, and showed a peak-to-peak voltage of 200 mV and -6 dB bandwidth of ~45%. The receiving element was excited by 1 μJ pulse and showed ~ 80 mVpp response and ~50% in -6 dB bandwidth, respectively (Figure 6).

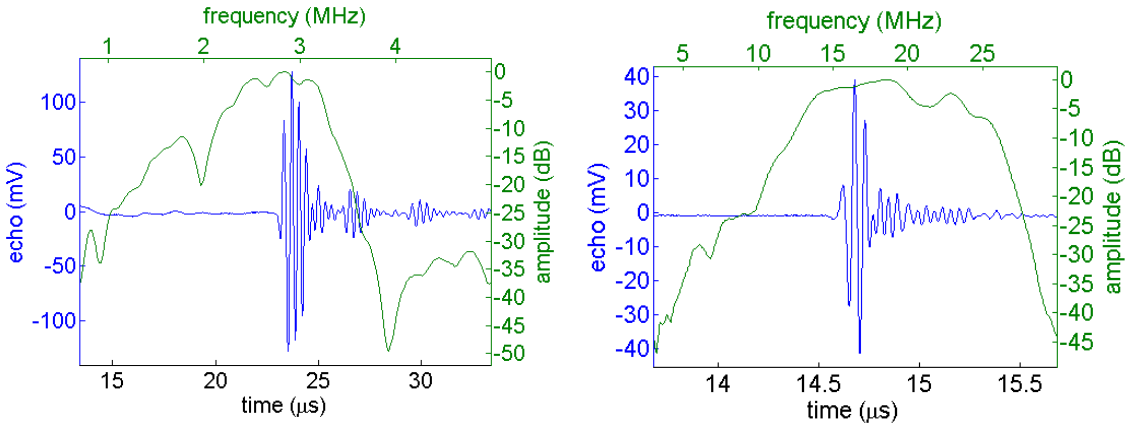

Figure 6. Pulse-echo response of full array elements at transmission (left) and receiving (right).

Based on these parameters, contrast imaging will be achievable at distance from the transducer ranging from 20 mm to 50 mm, which is the desired range of interest for transrectal ultrasound.

Task 4 Prepare manuscript for data dissemination (Months 30-33)

After completion and characterization of the prototype array transducer, data will be presented in a manuscript for a peer-reviewed journal such as IEEE Ultrasonics, Ferroelectrics, and Frequency Control.

We have completed publication of two refereed journal publication as well as three conference proceedings on the technology developed in years 1-2.

J. Kim, S. Li, S. Kasoji, P. A. Dayton and X. Jiang, "Phantom evaluation of stacked-type dual-frequency 1-3 composite transducers: a feasibility study on intracavitary acoustic angiography", Ultrasonics, Volume 63, December 2015, Pages 7–15.

K. H. Martin, B Lindsey, J Ma, M. Lee, F. S. Foster, X Jiang, P. A. Dayton, "Dual-frequency Transducers for Contrast Enhanced Ultrasound Imaging", *Sensors*, 2014 Nov 4;14(11):20825-42

J. Kim, S. Li, S. Kasoji, P. A. Dayton, and X. Jiang, "Dual-frequency super harmonic imaging piezoelectric transducers for transrectal ultrasound," in SPIE Smart Structures and Materials+ Nondestructive Evaluation and Health Monitoring, 2015, pp. 943823-943823-10.

J. Kim, S. Li, X. Jiang, S. Kasoji, and P. Dayton, "Development of transmitters in dual-frequency transducers for interventional contrast enhanced imaging and acoustic angiography," in Ultrasonics Symposium (IUS), 2014 IEEE International, 2014, pp. 679-682.

S. Li, W. Chang, W. Huang, and X. Jiang, "40-MHz Micromachined PMN-PT Composite Ultrasound Array for Medical Imaging," in ASME 2015 International Mechanical Engineering Congress and Exposition, 2015

Task 5 In-vitro testing of dual frequency PC-MUT co-linear array (Months 21-30)

Subtask 5.1 Tissue phantom testing (Months 21-25)

Gelatin based tissue mimicking phantoms will be used with a range of spherical hyperechoic and hypoechoic lesions. A spectrum of lesion detectability parameters will be tested. These lesions will be imaged at several axial depths using our prototype array and the Siemens EV-8C4 clinical TRUS probe. A blinded reader study will be performed and accuracy of the manually defined regions will be assessed between clinical and prototype probes for depth, phantom parameters, and imaging system parameters. Signal to noise ratio will be determined as a function of axial depth into tissue.

Subtask 5.2 Microvascular flow phantom testing (Months 25-30)

Images will be acquired in DFUB mode of microvascular flow phantoms with various diameters. Sinusoidal microvascular phantoms will be imaged at multiple axial depths, as well as with varying flow rates appropriate for simulating tumor microenvironment. A blinded reader study

will be performed in which readers rank the sensitivity to slow flow within an added tissue clutter background.

Methods and Results for Task 5:

Preparation of imaging phantoms and single element imaging tests

A tissue-mimicking phantom was prepared for contrast imaging studies. The graphite-gelatin phantom composed of 92.5% de-ionized water, 5% n-propanol (to adjust for speed of sound), 2.5% Kodak Photo-Flo 200 (surfactant), 7.5% g/mL porcine gelatin, and 0.115 g/mL graphite. The concentration of graphite was chosen to match experimental attenuation data of normal human prostate of 0.75 dB/cm/MHz. The ingredients were mixed with a stir bar over a stir plate and simultaneously heated to 40-45°C. Once the liquid phantom cooled back down to 30°C, it was poured into the custom mold and refrigerated for 24 hrs. The design of the mold consisted of two parallel cellulose tubes suspended in a hollow rectangular cup, such that if the opening of the cup faced up, the tubes ran parallel to the ground. The cellulose tubes were bonded to a larger diameter polyethylene tube using a water-proof adhesive. The distance from the cellulose tube to the surface of the phantom was approximately 5mm, with the tubes being in a distance of 5mm from each other.

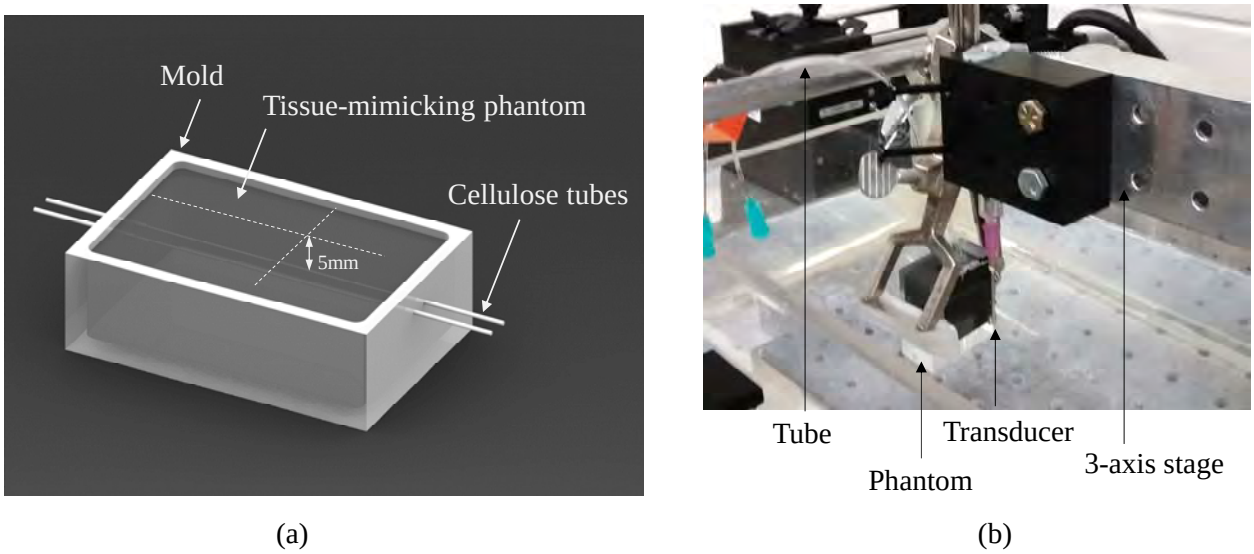

Figure 7. Design of a tissue-mimicking phantom (left) and photograph of phantom test setup.

The tissue-mimicking phantom was used for both microbubble signal detection and phantom blood vessel imaging (Figures 7, 8). The transducer was positioned at 8 mm away from the tissue phantom surface (approximately 13 mm away from the tubes). The 8 mm distance was selected as approximately twice of the estimated far field distance of the transmitter (4 mm) to avoid pressure fluctuation in the near field region. For microbubble signal detection, only one cellulose tube was used, and three different scenarios were considered including the cellulose tube filled with air, de-ionized water, and microbubbles. The stock microbubble solution was 10^{10} microbubbles/ml (a standard concentration in commercial agents) and the solution was diluted

1:100 in saline. In each case, the received signals were processed to obtain the frequency spectrum, and band-pass filtered with a frequency window of 10 to 15 MHz by using a 5th order Butterworth filter (MATLAB, Mathworks Inc., Natick, MA) to obtain the higher-harmonic content of the signals. When the cellulose tube was infused with microbubbles, signal-to-noise ratio (SNR) and CTR were calculated using following equations:

$$SNR = 20 \cdot \log\left(\frac{V_{\text{bubble}}}{V_{\text{noise}}}\right) \quad (1)$$

$$CTR = 20 \cdot \log\left(\frac{V_{\text{bubble}}}{V_{\text{tissue}}}\right) \quad (2)$$

where V_{bubble} denotes the detected peak voltage amplitude from microbubbles, and V_{tissue} and V_{noise} are the peak voltage amplitude detected from the tissue-phantom and water, respectively.
When performing superharmonic imaging tests, 2D images of the tissue-phantom with microbubbles flowing through the cellulose tubes were acquired. The transducer was 13 mm away from the tubes and scanned along the lateral axis in 500 μm increments using a 3-axis linear motion stage. Both cellulose tubes were infused with microbubbles simultaneously during the linear scanning using a syringe pump set an infusion rate of 50 μL/min. The function generator and RF power amplifier used for testing the pressure output were used for the superharmonic imaging tests (300 mVpp and 60 dB gain, in Figure). One- and two-cycle sinusoidal inputs at 2 MHz were applied, respectively, and SNR, CTR and -6 dB axial resolution under different input conditions were obtained and compared. The received microbubble signals were high-pass filtered at 10 MHz using a HC7 filter (TTE Filters, LLC., Los Angeles, CA) to eliminate the fundamental and lower-order harmonic responses (< 5th harmonic) from the tissue phantom. 100 A-lines acquired using a broadband receiver (BR-640, RITEC Inc. Warwick, RI) with a 16 dB gain were individually stored using an analog-to-digital converter (National Instruments, Austin, TX) and converted to B-mode images offline.

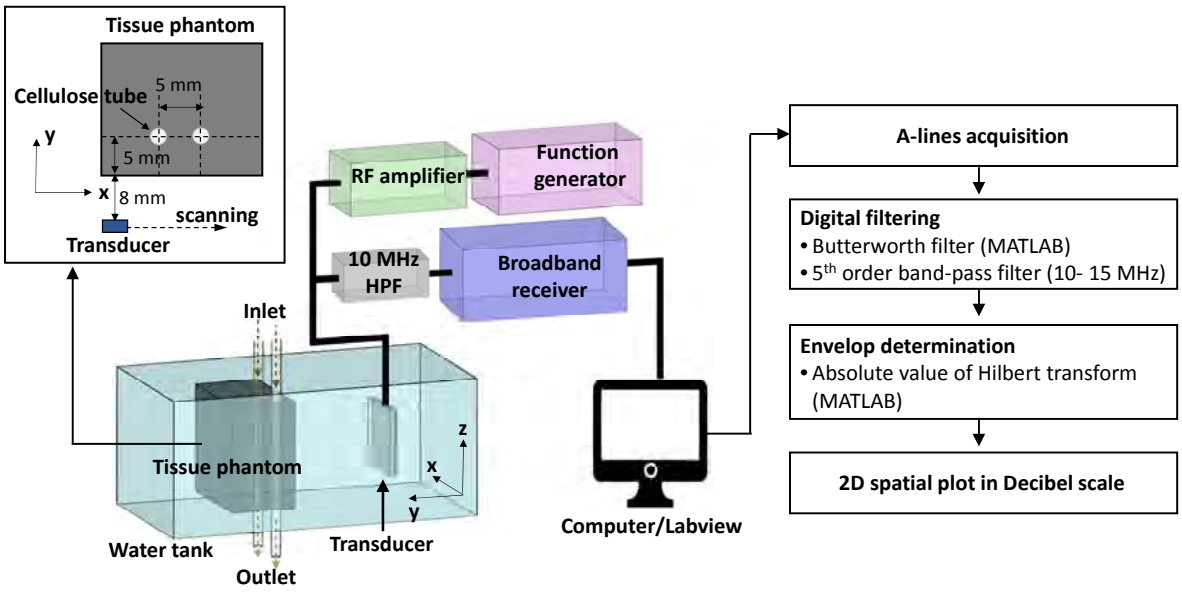

Figure 8. Experimental setup and data processing steps for the microbubble detection test and superharmonic imaging with a tissue phantom.

The cellulose tubes in the tissue-mimicking phantom were scanned by the aforementioned dual frequency imaging procedure. The results show that the superharmonic images obtained by our dual-frequency transducer clearly visualize the cross-section of tubes filled with microbubbles (Figure 9). In both images, a faint horizontal line is visible at approximately 6 mm in depth and it was generated by the electrical excitation from the function generator. The 1-cycle excitation waveform produced an averaged SNR and CTR of 16 dB, whereas the 2-cycle excitation waveform yielded SNR and CTR of 19 dB and 5 dB, respectively. The 3 dB higher SNR produced by the 2-cycle excitation compared to the 1-cycle excitation is attributed to a 67% stronger microbubble harmonic response, which is caused by the increased MI (from 1.39 to 1.63). On the other hand, the 11 dB decrease in CTR with the 2-cycle excitation is due to the higher frequency harmonic response (10 to 15 MHz) from the tissue-phantom boundary. This tissue-response generates a distinguishable line at a distance of 8 mm in Fig. 4 (b). The -6 dB axial resolution for the 1-cycle and 2-cycle excitations were measured to be 615 μm (5.5λ of 14 MHz waves) and 1.1 mm (10.2λ of 14 MHz waves), respectively. As predicted based on the enveloped amplitude results, the extended pulse length of microbubbles due to the increased pulse length of the 2-cycle excitation, reduces the quality of microcellulose tube images.

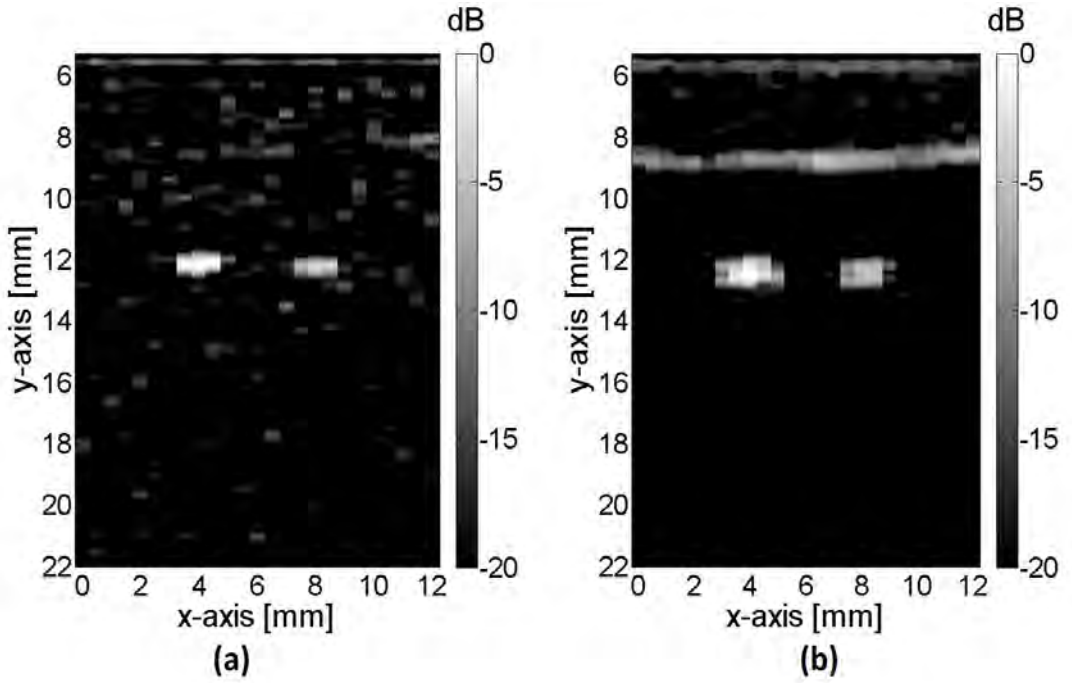

Figure 9. Superharmonic B-mode images of microtubes in a tissue-mimicking phantom using the prototype dual-frequency transducer by applying sinusoidal excitation at 2 MHz and receiving harmonic responses in the frequency range of 10 to 15 MHz; (a) 1-cycle excitation, (b) 2-cycle excitation.

Sub Array Real-time bubble contrast test

When performing superharmonic imaging tests, 2D images with microbubbles flowing through the cellulose tubes (Figure 10) were acquired. The transducer was placed 30 mm away from the tubes and a linear motor was used to scan the transducer along the lateral axis. The selection of 30 mm distance is the interest zone of prostate scanning range in the clinical study, which would make the test results meaningful. Initially in the test, the cellulose microtube was filled with the pure air, and probe was operated under high frequency B mode. Based on this setup, the image results shows the position of the tube, and enable for distance adjustment. After the tube was located and positioned appropriately, the contrast image test was performed. The cellulose tube was infused with microbubbles simultaneously during the scanning using a syringe pump setting an infusion rate of 5 mL/hr. The array ultrasound was operated at contrast mode (transmit at low frequency and receive at high frequency). By using Verasonics system (Verasonics, Redmond, WA), each single element could both excites and receives individually. Due to the pitch size of transmit and receive elements are relatively large (~ 2 wavelength in water), the system drove the probe in linear array mode. To excite the bubble signal, the excitation voltage is 55 V. For receiving element, the system acquired the RF signal and process band pass filtered (built-in 8 – 16 MHz).

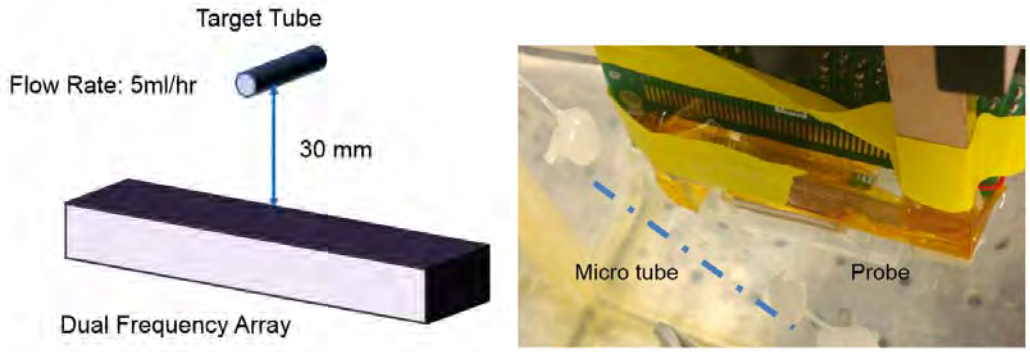

Figure 10. Schematic (left) and photograph (right) of a cellulose tube positioned relative to the array and the test set up.

The imaging result is presented in Figure 11. The left one shows the high frequency B-mode imaging of the microtube filled with air. The diameter of the cellulose tube is 200 μm, and the target is ~ 30 mm away from the ultrasound probe. From the result, a bright dot was observed, which presents the size and location of the micro tube. The second scenario is to perform the contrast mode. The array was operated with transmit at low frequency and receive at high frequency. The cellulose tube was injected with micro bubbles solution with the flow rate of 5μL/hr. After the fundamental frequency component was completely removed from receiving signals, only the filtered microbubble signal exhibited high-frequency harmonics. A single line of bubble signal was picked and the CNR was calculated to be ~18 dB. Overall, the superharmonic responses of the microbubbles (4^{th} to 6^{th} order harmonics) were successfully detected with a penetration depth of about 30 mm.

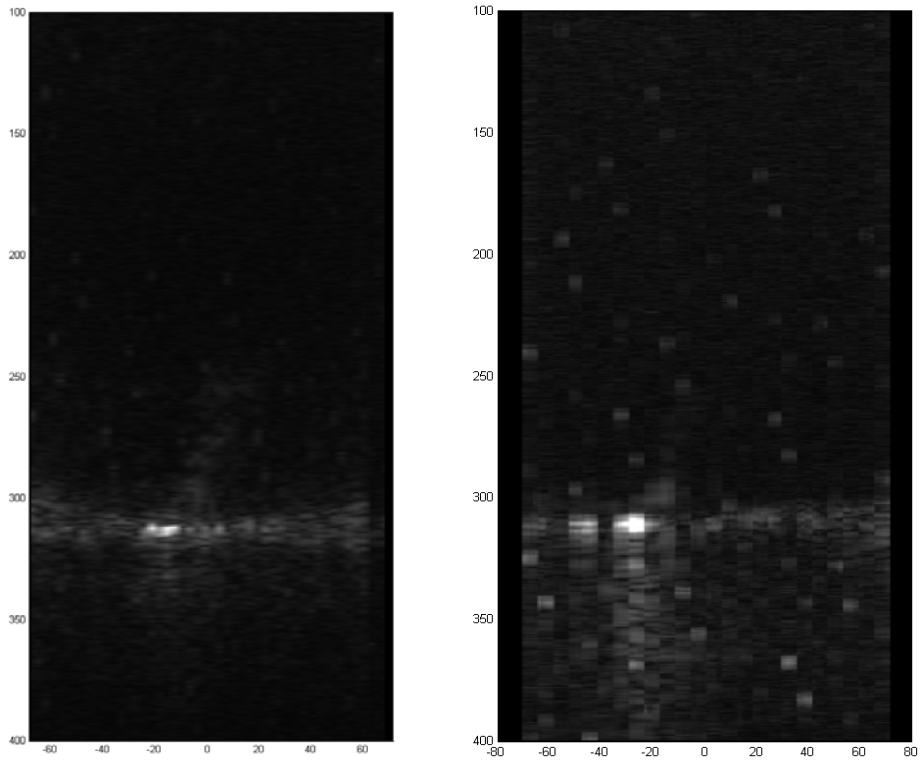

Figure 11. Sub-array imaging with pure air flow in micro-tube (high frequency B-mode) for positioning and micro bubble flow in cellulose tube (transmit low and receive high contrast mode).

Task 6 In-vivo testing of dual frequency PC-MUT co-linear array (Months 1-6, and 24-36)

Subtask 6.1 Prepare for IACUC approval for animal studies (Months 1-6)

Immediately upon project commencement, an appropriate protocol will be prepared for the University of North Carolina *Institutional Animal Care and Use Committee*, for eventual in-vivo imaging studies.

Subtask 6.2 Establish Dunning/Copenhagen rodent prostate cancer model (Months 24-27)

The Dunning R3327 cell line is available from ATCC, from the Johns Hopkins Collection. Twenty 60 day old male Copenhagen Rats (Harlan Indianapolis, IN) will be utilized for in-vivo imaging. Cells will be propagated in culture, and then subcutaneously injected into the flank of each rat. Imaging will be performed starting one week after implantation, and continued until tumors reach approximately 15 mm in diameter, after which animals will be humanely euthanized. For all procedures, animals will be anesthetized using inhaled oxygen and 2% isoflurane. Body temperature will be maintained using a temperature controlled heating pad.

Subtask 6.3 Assess performance of imaging probe in animal model (Months 25-36)

The diagnostic utility of the prototype array to detect cancerous lesions will be assessed in vivo in terms of spatial and temporal sensitivity relative to a conventionally used clinical probe. Two specific imaging approaches will be assessed – ultrasound molecular imaging and microvessel mapping. Spatial sensitivity will be determined by how accurately molecularly targeted contrast agents and microvascular abnormalities conform to the tumor boundaries (relevant to improving biopsy guidance accuracy), while temporal sensitivity will be assessed by observing how these metrics evolve throughout the course of a tumor's growth. The Dunning model will be established in the right flank of 20 male rats (the left flank will serve as a control). To assess the imaging performance of the prototype array as a function of axial depth between 0.5 and 5 cm, tissue mimicking gelatin standoffs will be inserted between the animals' skin and transducer to simulate a deeper lesion depth. Images will be acquired with the clinical probe for contrast imaging of the same tumor and control tissue volumes to compare molecular imaging signal strengths and ability to visualize vascular abnormalities.

Our team has not completed the in-vivo imaging to during year three due to some unexpected delays in the array fabrication and testing. These delays were primarily due to in-house fabrication of the interconnects. This challenge was solved by working with a commercial vendor to provide this intricate custom part. We have completed Subtask 6.1, preparation of an IACUC animal protocol, however Subtasks 6.2 and 6.3 will be completed in the EWOF period.

Task 7 Prepare manuscript for data dissemination (Months 30-36)

An additional 1-2 publications are anticipated to be completed during the EWOF period based in-vivo imaging studies.

Key Year 3 Research Accomplishments

- A 24/96-element dual-frequency 2 MHz/20 MHz linear array transducer has been designed and fabricated, and the initial tests have demonstrated promising performance.

Conclusion

Several iterations of dual frequency transducers designed for transrectal ultrasound imaging have been successfully prototyped and tested. The main accomplishment in year three was the fabrication and testing of the full dual frequency linear array. The design, fabrication, and testing of this array was really the focus of this entire project. Our prototype consists of 24 elements for transmission at 2 MHz and 96 elements for reception at 20 MHz. It is currently the only dual-frequency linear array of this frequency range in existence. Data suggests it should enable superior contrast imaging to current single-frequency arrays, thereby improving our ability to resolve cancer-associated angiogenesis in the prostate. Electrical impedance and primary acoustic tests have been performed. The low frequency transmission elements were excited by 200 V pulse, and showed a peak-to-peak voltage of 70 mV and -6 dB bandwidth of ~45%. The receiving elements were excited by 1 μJ pulse and showed ~ 300 mV_{pp} response and ~50% in -6 dB bandwidth, respectively. Although some initial testing has been completed, what remains is final optimization and in-vivo imaging. Over the past year, our progress was set back by some challenges in the array fabrication, which we hope we have resolved. A request for Extension Without Funds has been submitted and we hope to complete the final array optimization and validation of in-vivo imaging during the EWOF project year.

Publications and Abstracts

Abstract/Presentations

J. Kim, S. Li, S. Kasoji, P. A. Dayton, and X. Jiang, "Dual-frequency super harmonic imaging piezoelectric transducers for transrectal ultrasound," in SPIE Smart Structures and Materials+ Nondestructive Evaluation and Health Monitoring, 2015, pp. 943823-943823-10.

J. Kim, S. Li, X. Jiang, S. Kasoji, and P. Dayton, "Development of transmitters in dual-frequency transducers for interventional contrast enhanced imaging and acoustic angiography," in Ultrasonics Symposium (IUS), 2014 IEEE International, 2014, pp. 679-682.

S. Li, W. Chang, W. Huang, and X. Jiang, "40-MHz Micromachined PMN-PT Composite Ultrasound Array for Medical Imaging," in ASME 2015 International Mechanical Engineering Congress and Exposition, 2015

Publications

J. Kim, S. Li, S. Kasoji, P. A. Dayton and X. Jiang, "Phantom evaluation of stacked-type dual-frequency 1-3 composite transducers: a feasibility study on intracavitary acoustic angiography", Ultrasonics, Volume 63, December 2015, Pages 7–15.

K. H. Martin, B Lindsey, J Ma, M. Lee, F. S. Foster, X Jiang, P. A. Dayton, “Dual-frequency Transducers for Contrast Enhanced Ultrasound Imaging”, *Sensors*, 2014 Nov 4;14(11):20825-42

Inventions, Patents, and Licenses

Nothing to report

Reportable Outcomes

Nothing to report

Other Achievements

Nothing to report

References

N/A

Appendices

Nothing to report